

Timing Acquisition for Wavelet-Based Multirate Transmissions

†Chih-Ming Fu, ‡Wen-Liang Hwang and †Chung-Lin Huang

†Department of Electrical Engineering, National Tsing Hua University, Taiwan

‡Institute of Information Science, Academia Sinica, Taiwan

Abstract—The acquisition problem in wavelet-based modulation is very important. We discuss the problem of the ML-based method proposed in [1] for timing acquisition and then we develop a novel acquisition algorithm. Our method uses the properties of the scaling function in the derivation of the acquisition function. We also show that the S-curve of our acquisition algorithm is smooth and has a unique zero during the signaling interval. Thus, we can acquire the correct symbol timing without ambiguity. The performance of our acquisition algorithm is evaluated by Monto-Carlo simulation using Meyer wavelet.

I. INTRODUCTION

A transmission system that employs wavelets as signaling waveforms result in a multirate environment [1]. A few examples of the use of wavelets over time-varying channels are shown in [2][3][4]. The implementations and performances of multirate transmission systems operating over noisy channels are discussed in [5]. The important synchronization problem is studied in [1], where the ML-based method was proposed by using orthogonal wavelets to synchronize a multirate system. However, the drawback of this ML-based approach lies in that it can not be used for timing acquisition. Because of the oscillation of wavelets, this approach produces many spurious local maxima within a signaling interval in its ML-function. As a consequence, a small jittering in acquisition process may lead to a wrong timing point.

We propose a novel timing acquisition algorithm that can acquire the correct timing of a multirate system. Our approach is based on applying the ML-based method to the signal after it is projected to the space spanned by the scaling function. Because that the scaling function has less oscillations than a wavelet and the orthogonality between the scaling function and the wavelets, our synchronization function, given in (12), that is derived from the signal projected onto the scaling function space is a smooth curve with only one zero crossing within a signal interval. Thus, we can use the traditional closed-loop techniques in acquiring the correct timing point without any ambiguity.

The paper is organized as follows. In section II, we review the previous work [1], a popular synchronization technique by means of ML methods using wavelets. We also discuss the problems of this synchronization method if it were used for timing acquisition. In section III, we introduce our acquisition method and derive the function used for acquisition. We also show the performance of our acquisition algorithm by

measuring the mean acquisition time. Finally, in section IV, we give our conclusions.

II. SYSTEM DESCRIPTION AND TRADITIONAL SYNCHRONIZATION TECHNIQUE

In this section, we review the synchronization technique proposed in [1] for a wavelet-based multirate communication systems. In the following, we limit ourselves to the aspect of data symbol synchronization, assuming either that carrier frequency and phase are exactly recovered prior to clock extraction or that the transmission is baseband.

A. System Model

A multirate waveform is defined as the superposition of M different signal components, each supporting a different data rate and occupying a different spectrum segment (*subband*) as follows

$$s(t) = A \sum_{m=0}^{M-1} \sum_n d_{m,n} \psi_{m,n}(t), \quad (1)$$

where A is a positive amplitude factor, $d_{m,n} \in \{\pm 1\}$ are independent, identically distributed binary data symbols—the *translation* and *scale* index n , m denote the n th symbol of the m th subband—and $\psi_{m,n}(t)$ is a scaled and translated version of the real-valued *mother wavelet* $\psi(u)$

$$\psi_{m,n}(t) = 2^{m/2} \psi\left(\frac{2^m}{T_0} t - n\right). \quad (2)$$

The signaling interval $T_0/2^m$ in the m th subband is related to the signaling interval T_0 at the slowest subband. The inner product between $\psi_{m,n}(t)$ and $\psi_{p,q}(t)$ satisfies the orthogonal property

$$\frac{1}{T_0} \int_{-\infty}^{\infty} \psi_{m,n}(t) \psi_{p,q}(t) dt = \delta_{m,p} \delta_{n,q}. \quad (3)$$

We can write the received waveform for the additive white Gaussian noise (AWGN) channel as

$$r(t) = s(t - \tau) + w(t), \quad (4)$$

where $s(t)$ is given in (1), $\tau \in [0, T_0)$ denotes the channel delay to be estimated by a receiver, and $w(t)$ is AWGN with two-sided power spectral density $\sigma_w^2 = 1/2N_0$. If there were a timing error, the samples would be affected by inter symbol interference (ISI) arising from different subbands, because the orthogonality between bases would be lost.

B. NDA-ML Synchronizer

Our aim in this section is to discuss the problems of the nondata-aided (NDA) (or blind) clock recovery algorithm for signal (4), based on ML estimation [1]. We will review this clock-recovery algorithm at first. The ML function for the estimation of the delay τ , based on the observation model (4), is

$$\Lambda(\mathbf{r}|\tilde{\tau}, \tilde{\mathbf{d}}) = \exp\left(\frac{2}{N_0} \int_{T_{obs}} r(t)s(t - \tilde{\tau})dt\right), \quad (5)$$

where $\tilde{\mathbf{d}}$ is the vector of data symbols belonging to all subbands, $\tilde{\tau}$ is the trial value of τ , and T_{obs} is the observation interval. The NDA-ML synchronizer proposed by [1] is used to maximize the ML function

$$F(\tilde{\tau}) = \sum_m F_m(\tilde{\tau}) = \sum_m \sum_n y_{m,n}(\tilde{\tau})^2, \quad (6)$$

where

$$y_{m,n}(\tilde{\tau}) = \frac{1}{T_0} \int_{T_{obs}} r(t)\psi_{m,n}(t - \tilde{\tau})dt. \quad (7)$$

The tracking of the clock timing of the received signal can be achieved by means of a feedback loop, where the error signal is

$$e_k = \sum_m \frac{d}{d\tilde{\tau}} [y_{m,k}(\tilde{\tau})^2]. \quad (8)$$

The discrete-time loop operation is governed by the conventional recursion

$$\hat{\tau}_{k+1} = \hat{\tau}_k - \gamma T_0 e_k, \quad (9)$$

where $\hat{\tau}_k$ denotes the timing estimate at the k th step, e_k is the loop error signal, and γ is the algorithm step size.

Fig.2 shows the simulation of the function $F_m(\tilde{\tau})$ and $F(\tilde{\tau})$ without additive noise for three subbands modulation. Meyer wavelet used in this simulation is shown in Fig.1. The top three

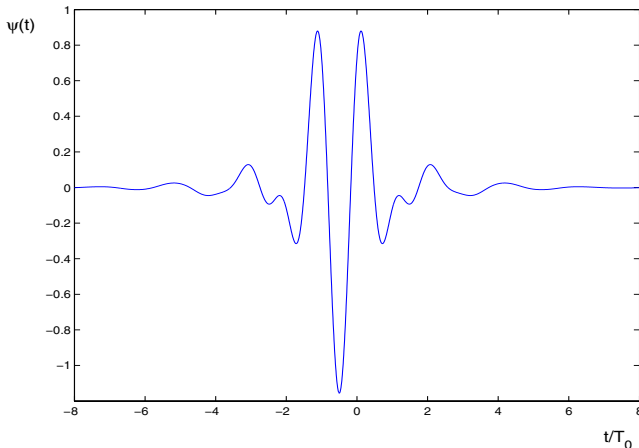


Fig. 1. Meyer wavelet.

figures in Fig.2 show $F_m(\tilde{\tau})$ in each subband and the bottom of the figure shows $F(\tilde{\tau})$. The scale in Fig.2 is normalized by T_0 such that the timing points for signal acquisition are at the integer points. The circle mark at each subband is the

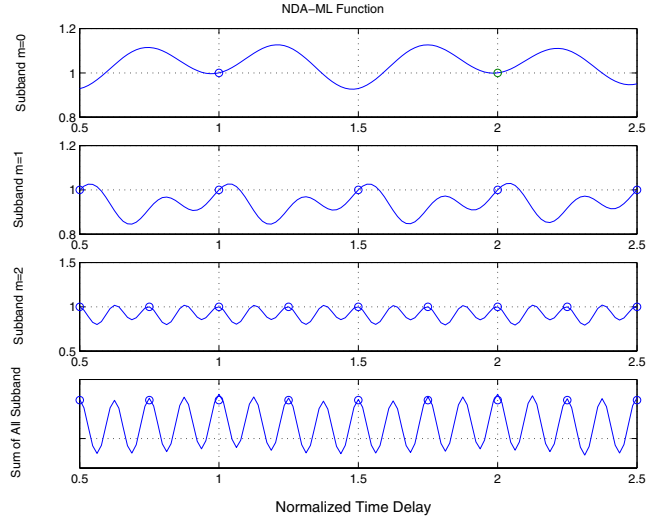


Fig. 2. Three-subband NDA ML function.

correct timing point for the subband. We will now discuss the problems with the ML-Based method. One can observe from the figure $F(\tilde{\tau})$ that there are many spurious local maxima between any two consecutive integer points in $F(\tilde{\tau})$. Since the integer points are the locations for our acquisition, using $F(\tilde{\tau})$ for acquisition may lead to wrong timing points. One can also observe that the function $F_m(\tilde{\tau})$ in each subband cannot be used for acquisition: either there are local maxima between consecutive integer points or the maxima are not at the integer points. The out-of-synchronization of $F_m(\tilde{\tau})$ is due to the inter-subband interference.

The problem cannot be solved by simply passing the function $F(\tilde{\tau})$ through a low-pass filter since the values of the spurious local maximum points are very close to the correct timing point. Therefore, the acquisition algorithm in [1] can not be used for timing acquisition. We need a new acquisition algorithm for wavelet-based multirate systems.

III. ACQUISITION USING SCALING FUNCTION

Here we will introduce a reliable method to acquire the symbol timing. Our method uses the property of scaling function in orthogonal wavelet theory. The scaling function $\phi_{m,n}(t)$ of an orthogonal wavelet has the property that

$$\frac{1}{T_0} \int_{-\infty}^{\infty} \phi_{m,n}(t)\psi_{p,q}(t)dt = 0, \quad \text{for } m \leq p. \quad (10)$$

where $\phi_{m,n}(t)$ is the scaling function and m, n, p, q are integers. The convolution between $\psi_{m,n}(t)$ and filter $\phi_{0,q}(-t)$ is

$$R_{m,n,0,q}\left(\frac{\hat{\tau}}{T_0}\right) = \frac{1}{T_0} \int_{T_{obs}} \psi_{m,n}(t)\phi_{0,q}(t - \hat{\tau})dt. \quad (11)$$

The mother scaling function used in our simulation is shown in Fig.3.

By projecting the received signal $r(t)$ into the space spanned by the scaling functions $\phi_{0,n}(-t)$, most of the self-noise in

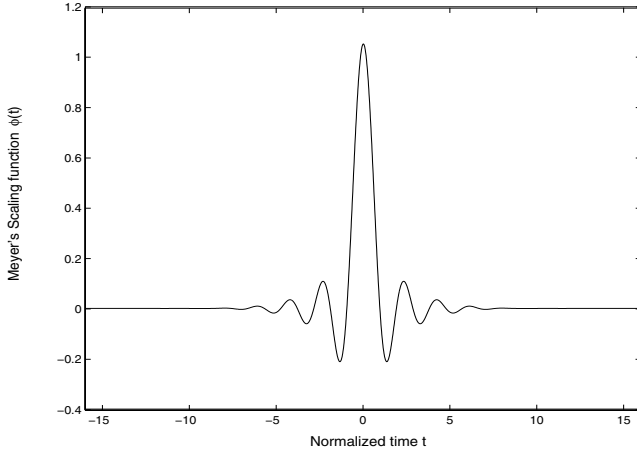


Fig. 3. Meyer scaling function.

the received signal will be removed. This property and the orthogonality between the wavelets and the scaling function at integer translations allow us to derive an ML-based acquisition function that is smooth and has the local maxima only at the integer points. We summarize the procedure of deriving our acquisition function as follows:

For simplicity, we define the normalized timing error

$$\hat{\theta} = (\hat{\tau} - \tau)/T_0.$$

We use the correlation function between wavelet function and scaling function $R_{m,n,0,q}$. The function $R_{m,n,0,q}$ is smooth and have only one zero point in signal interval T_0 . The function $R_{m,n,0,q}$ together with its derivative, we define our synchronization function to be

$$F(\hat{\theta}) = \sum_q f_q(\hat{\theta})f'_q(\hat{\theta}), \quad (12)$$

where $f_q(\hat{\theta})$ is the response of the filter $\phi_{0,q}(-t)$ to input $r(t)$. Although this function is given as the definition, the function can be derived with a similar approach as that in [1] on the received signal after it is projected to the space spanned by the scaling functions. By using equations (2), (12) and (11), we have

$$\begin{aligned} f_q(\hat{\theta}) &= \frac{1}{T_0} \int_{T_{obs}} r(t)\phi_{0,q}(t - \hat{\tau})dt \\ &= \frac{1}{T_0} \int_{T_{obs}} [s(t - \tau) + w(t)]\phi_{0,q}(t - \hat{\tau})dt \\ &= \sum_m \sum_n d_{m,n} R_{m,n,0,q}(\hat{\theta}) + z_q(\hat{\tau}), \end{aligned}$$

where

$$z_q(\hat{\tau}) \triangleq \frac{1}{T_0} \int_{T_{obs}} w(t)\phi_{0,q}(t - \hat{\tau})dt.$$

By using eq.(10), if the timing is synchronized, the synchronization function (12) at the integer point of $\hat{\theta}$ will be zero. Then, we can seek the zeros of $F(\hat{\theta})$ to locate the correct timing points. The symbol timing can be recovered by means

of a feedback loop where the error signal is generated. Let the error signal for our synchronizer $e_s(k)$ be defined as:

$$e_s(k) \triangleq f_k(\hat{\theta}_k)f'_k(\hat{\theta}_k). \quad (13)$$

The discrete-time loop operation is governed by the conventional recursion

$$\hat{\tau}_{k+1} = \hat{\tau}_k - \gamma T_0 e_s(k). \quad (14)$$

where γ is the algorithm stepsize. Fig.4 shows the structure of our method. The NCO is driven at the rate $1/T_0$. We note

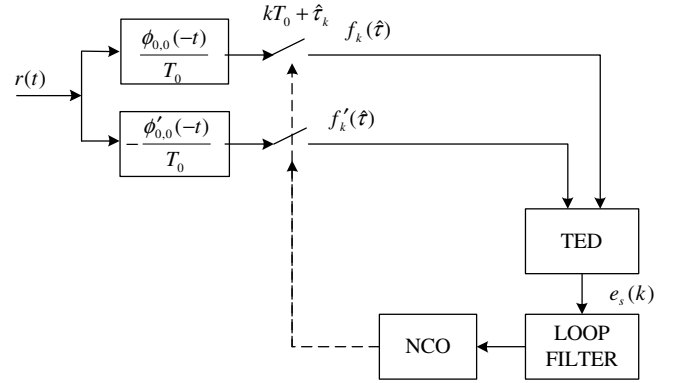


Fig. 4. Functional block diagram of clock synchronizer for slowest subband using $\psi_{0,0}(t)$.

that (14) can be reformulated in terms of normalized timing errors, i.e.,

$$\hat{\theta}_{k+1} = \hat{\theta}_k - \gamma e_s(k). \quad (15)$$

A. Performance Evaluation

We use the S-curve [6] to evaluate the performance of our method. The S-curve will show the dynamic acquisition property. We consider the loop S-curve, defined as

$$S(\theta) \triangleq E[e_s(k)|\hat{\theta}_k = \theta]. \quad (16)$$

The error $e_s(k)$ can be written as the sum of the S -curve plus a zero-mean disturbance:

$$e_s(k) = S(\hat{\theta}_k) + \nu_k(\hat{\theta}_k). \quad (17)$$

Let us consider the loop S-curve in (11) and (13) and derive

$$f_q(\hat{\theta}) = \sum_m \sum_n d_{m,n} R_{m,n,0,q}(\hat{\theta}) + z_q(\hat{\tau}) \quad (18)$$

$$f'_q(\hat{\theta}) = \sum_m \sum_n d_{m,n} R'_{m,n,0,q}(\hat{\theta}) + z'_q(\hat{\tau}), \quad (19)$$

where $R'_{m,n,0,q}(\hat{\theta}) \triangleq dR_{m,n,0,q}(\hat{\theta})/d\hat{\theta}$ is the response of $r(t)$ to the derivative filter of $\phi_{0,q}(-t)$, and $z_q(\hat{\tau})$ and $z'_q(\hat{\tau})$ are the respective responses of $w(t)$ to the derivative filter of $\phi_{0,q}(-t)$. Hence, by substituting (18) (19) in (13) for $\hat{\tau}_k = \hat{\tau}$ and rearranging yields

$$\begin{aligned} e_s(k) &= \left(\sum_m \sum_n d_{m,n} R_{m,n,0,k}(\hat{\theta}) + z_k(\hat{\tau}) \right) \\ &\cdot \left(\sum_{m'} \sum_{n'} d_{m',n'} R'_{m',n',0,k}(\hat{\theta}) + z'_k(\hat{\tau}) \right). \quad (20) \end{aligned}$$

To proceed further, assume zero-mean and independent symbols so that

$$E\{d_{p,q}d_{m,n}\} = \begin{cases} 1 & \text{if } p = m, q = n \\ 0 & \text{otherwise} \end{cases} \quad (21)$$

Using (16)(21) and taking expectation of $e_s(k)$, we have

$$S(\theta) = \sum_m \sum_n [R_{m,n,0,k}(\theta)R'_{m,n,0,k}(\theta)]. \quad (22)$$

Ignoring the recursion number k , the S-curve of our acquisition algorithm is shown in Fig.5. The curve varies smoothly.

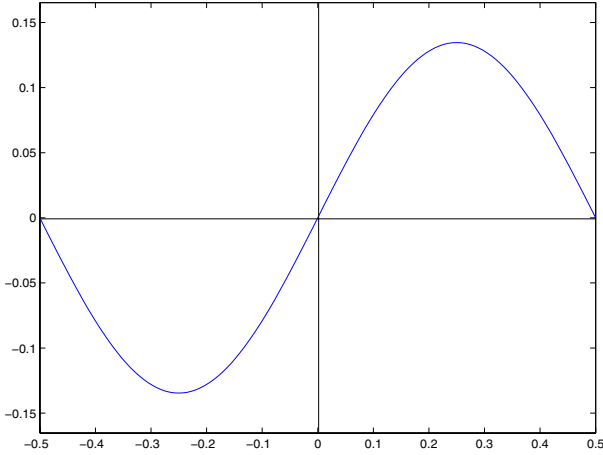


Fig. 5. The curve shows that we can find the timing in integer for three bands.

This means that the method we used will not have incorrect points at those that occurred in the ML-based method in [1]. The low-pass nature of filter $\phi_{0,q}(-t)$ is the point of the smoothness. The additional orthogonal relation between wavelet and scaling function is why we can acquire the timing. Using Meyer wavelet, the S-curve can be approximate to

$$S(\theta) = D_s \sin(2\pi\theta) \quad (23)$$

where $D_s = 0.13462$. For Daubechies 4th-order wavelet basis, we have $D_s = 0.3966$.

B. Mean Acquisition Time

The mean acquisition time is a measurement of our acquisition performance. The acquisition time is a random variable whose outcome depends on the noise level and the initial error $\hat{\theta}_0$. Briefly, if we neglect the noise term in (17) the timing error at the k -th step can be rewritten as

$$\hat{\theta}_{k+1} = \hat{\theta}_k - \gamma S(\hat{\theta}_k). \quad (24)$$

By using computer simulation, we find that the number of iteration needed to acquire the right timing with errors smaller than $10^{-3}T_0$ has a simple relationship with initial timing error $\hat{\theta}_0$, which is shown in Fig.6. The number of iteration to acquire timing depend on $D_s\gamma$. In other words the step size controls the speed of acquisition process. If we assume that the initial

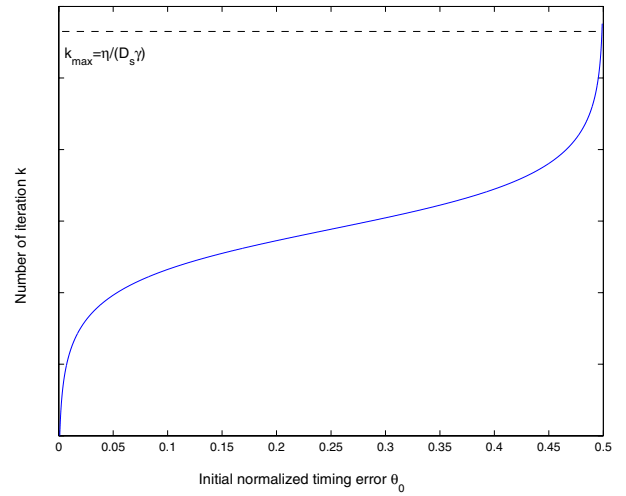


Fig. 6. The number of iteration to locate timing in different initial error θ .

error $\hat{\theta}_0$ is uniformly in $[0, T_0)$, our simulation shows that the mean acquisition time is

$$E[T_{acq}] \approx \frac{\eta T_0}{\gamma D_s}, \quad (25)$$

where η will vary from 1.5 to 2.5 for $D_s\gamma$ in the range $[10^{-1}, 10^{-5}]$.

C. Simulation Result

The performance of our method is evaluated by Monto-Carlo simulation using Meyer wavelet. Now, we can acquire the timing of each subband and then track the symbol timing of the received signal. Fig.7 shows our method to acquire the correct timing, and continue tracking the timing, where B_n is the effective noise bandwidth. Fig.8 shows normalized error deviation of our method for the three-subbands case in different E_b/N_0 , where E_b is the energy of each data symbol. After the signal is acquired, the method proposed in [1] can

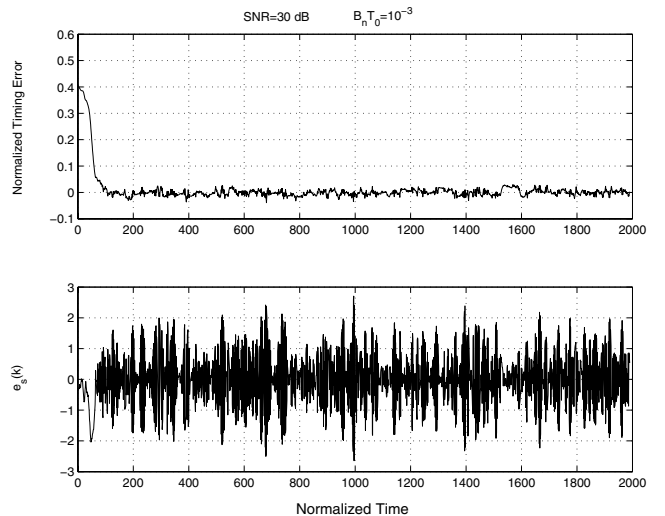


Fig. 7. The regression of normalized clock error $\hat{\theta}$, $\gamma = 300$.

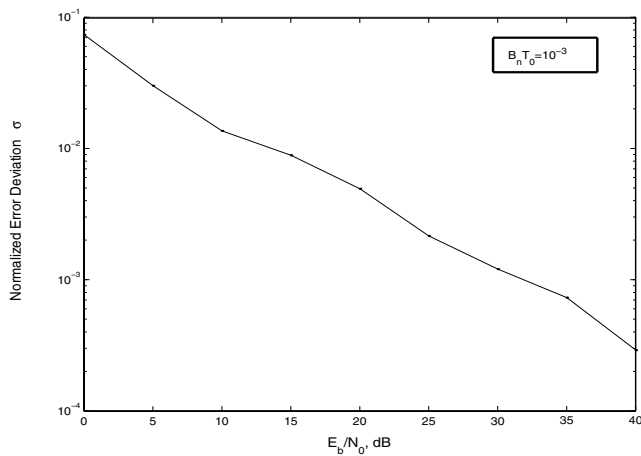


Fig. 8. Normalized error deviation for the three-subband Correlation Method clock synchronizer.

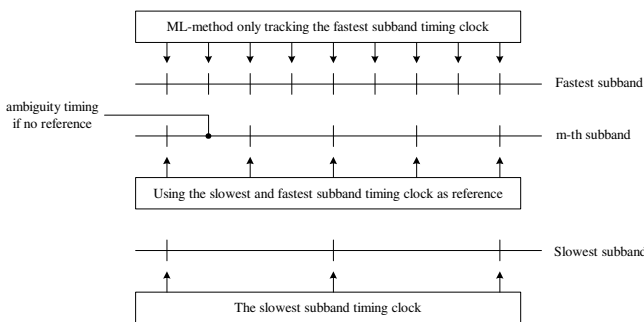


Fig. 9. Find the timing clock of m th subband from the slowest subband.

then be applied for tracking or using the slowest-band timing information to locate the timing for the next faster band by dividing the timing of the slowest band by half. Note that there is an ambiguity in selecting which points to drop when the timing of a slower subband is obtained from that of a faster subband. We construct a new structure to locate each subband timing as shown in Fig.9.

IV. CONCLUSION

The acquisition problem in wavelet-based modulation is very important. The ML-based method proposed in [1] cannot be used in timing acquisition. Before it can be used for tracking the symbol timing, we need to develop an acquisition algorithm. We propose a novel acquisition method that uses explicitly the scaling function in the derivation of our acquisition function. The S-curve of our acquisition function is smooth and has a unique zero during the signaling interval. Thus, we can acquire the correct symbol timing without ambiguity.

REFERENCES

[1] M. Luise, M. Marselli, and R. Reggiani, "Clock synchronization for wavelet-based multirate transmissions," *IEEE Trans. on Commun.*, vol. 48, pp. 1047–1054, June 2000.
 [2] G. Wornell, "Emerging applications of multirate signal processing and wavelets in digital communications," *Proc. IEEE*, vol. 84, pp. 586–603, Apr. 1996.

[3] C. M. Fu, W. L. Hwang, and C. L. Huang, "Clock synchronization for fractal modulation," *IEEE ICASSP*, pp. 2810–2812, 2002.
 [4] G. Wornell and A. V. Oppenheim, "Wavelet based representations for a class of self similar signals with applications to fractal modulation," *IEEE Trans. on Inform. Theory*, vol. 38, pp. 785–800, May 1992.
 [5] L. Atzori, D. D. Giusto, and M. Murrioni, "Performance analysis of fractal modulation transmission over fast-fading wireless channels," *IEEE Trans. on Broadcasting*, vol. 48, pp. 2813–2816, 2002.
 [6] U. Mengali and A. N. D'Andrea, *Synchronization Techniques for Digital Receivers*, Plenum press . New York and London, 1997.